# Improved numerical modelling of surface tension effects via a novel discretization of the Continuum Surface Force model

C A Batha

Chris.Batha@awe.co.uk

AWE, Reading, Berkshire, UK*.

## Contents

1. Motivation

2. Numerical method overview

3. Numerical examples

4. Conclusions

## Motivation

The CSF model reformulates the discontinuous jump conditions at fluid interfaces, due to surface tension, as a smoothly varying volume force acting over the fluid interface.

The imbalance between surface tension forces and associated pressure gradients in the CSF model generates spurious velocities, at fluid interfaces.

A numerical technique is presented in which the only potential source of 'spurious currents' lies in curvature estimation.

The method is a member of the class of balanced force algorithms [2].

## General numerical method overview

The method is currently implemented in a 2D compressible Lagrange-Remap multi-component , single pressure model, hydrocode.

Youngs' Volume of fluid method [5] used to track interfaces.

Numerical method includes

- Orthogonal curvilinear metric:

$$dS^2 = h_1^2\, dx_1^2 + h_2^2\, dx_2^2 + h_3^2\, dx_3^2. \tag{1}$$

- Collocated grid

## General numerical method overview cont

- Unsplit Lagrange phase
- Directionally split Van Leer remap method
- Simplified compressible flow model; an internal energy equation is evolved for each fluid component.

CSF discretization itself is fully applicable to 3D problems, though for ease of description the 2D analogue is given here.

## Novel CSF discretization

Consider a four cell stencil, centered on vertex (i,j), containing two fluids, with volume fractions $f_1$ , $f_2 = 1 - f_1$, separated by an interface.

In the presence of surface tension there is a pressure jump at the interface such that fluids have pressures $p_1$, $p_2$.

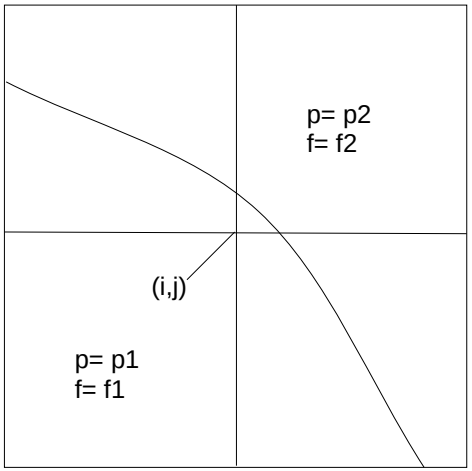

## Novel CSF discretization cont

Cell centered pressures, in terms of fluid pressures and volume fraction of fluid 1, $f_1$ in the cell stencil used are given as

$$p_{i-\frac{1}{2},j-\frac{1}{2}} = f_{i-\frac{1}{2},j-\frac{1}{2}}\, p_1 + (1 - f_{i-\frac{1}{2},j-\frac{1}{2}})\, p_2, \tag{2}$$

$$p_{i-\frac{1}{2},j+\frac{1}{2}} = f_{i-\frac{1}{2},j+\frac{1}{2}}\, p_1 + (1 - f_{i-\frac{1}{2},j+\frac{1}{2}})\, p_2, \tag{3}$$

$$p_{i+\frac{1}{2},j-\frac{1}{2}} = f_{i+\frac{1}{2},j-\frac{1}{2}}\, p_1 + (1 - f_{i+\frac{1}{2},j-\frac{1}{2}})\, p_2, \tag{4}$$

$$p_{i+\frac{1}{2},j+\frac{1}{2}} = f_{i+\frac{1}{2},j+\frac{1}{2}}\, p_1 + (1 - f_{i+\frac{1}{2},j+\frac{1}{2}})\, p_2. \tag{5}$$

The forces on cell vertex (i,j), due to cell pressure are thus,

- In the axial direction

$$\frac{1}{2}A_{i,j+\frac{1}{2}}\left(p_{i-\frac{1}{2},j+\frac{1}{2}}-p_{i+\frac{1}{2},j+\frac{1}{2}}\right)+\frac{1}{2}A_{i,j-\frac{1}{2}}\left(p_{i-\frac{1}{2},j-\frac{1}{2}}-p_{i+\frac{1}{2},j-\frac{1}{2}}\right) \tag{6}$$

- In the radial direction

$$\frac{1}{2}A_{i-\frac{1}{2},j}\left(p_{i-\frac{1}{2},j+\frac{1}{2}}-p_{i-\frac{1}{2},j-\frac{1}{2}}\right)+\frac{1}{2}A_{i+\frac{1}{2},j}\left(p_{i+\frac{1}{2},j+\frac{1}{2}}-p_{i+\frac{1}{2},j-\frac{1}{2}}\right) \tag{7}$$

- Where cell face areas are given by

$$(dA)_{i,j\pm\frac{1}{2}}=(h_1\,h_3\,dx_1\,dx_3)_{i,j\pm\frac{1}{2}},\quad (dA)_{i\pm\frac{1}{2},j}=(h_2\,h_3\,dx_2\,dx_3)_{i\pm\frac{1}{2},j}. \tag{8}$$

In a static frame the balance of forces due to pressure and surface tension is described by the Laplace-Young law, where $\sigma$ & $\kappa$ denote surface tension coefficient and interfacial curvature,

$$\Delta p = (p_1 - p_2) = \sigma\kappa. \tag{9}$$

In equilibrium,the force on vertex (i,j) due to surface tension

$$(\mathbf{F}_m)_{i,j} = (\sigma\kappa)_{i,j} \left[ \left( \frac{A\delta f}{V} \right)_m \right]_{i,j} \text{ for } m = 1, 2 \tag{10}$$

Where, in terms of the metric

$$\left( \frac{A\delta f}{V} \right)_m \approx \frac{1}{h_m} \frac{\partial f}{\partial x_m}. \tag{11}$$

If the exact curvature is known (11) ensures exact equilibrium, eliminating spurious velocities by design.

## Numerical curvature estimation

Three main techniques investigated for estimating interfacial curvature

- Finite differencing of a convolved volume fraction: CVF
- Finite differencing of Youngs' normal vectors [5] : Youngs
- Differentiating a Height Function [2] : HF

## Numerical curvature estimation: CVF

Volume fraction field convolved using smoothing kernel

$$\hat{f}_{j,k} = \frac{\sum_{l,m} f_{j,k} K(|X_{j,k} - X_{l,m}|, \gamma) dx_1 dx_2}{\sum_{l,m} K(|X_{j,k} - X_{l,m}|, \gamma) dx_1 dx_2} \tag{12}$$

Where $\gamma$ is a smoothing scale and $K(r, \gamma)$ is the following simple cubic kernel

$$K(r,\gamma) = \begin{cases} \left(1 - 6\left(\frac{r}{\gamma}\right)^2 + 6\left(\frac{r}{\gamma}\right)^3\right) & \text{if } 2r < \gamma \\ 2\left(1 - \left(\frac{r}{\gamma}\right)\right)^3 & \text{else if } r < \gamma \\ 0 & \text{otherwise} \end{cases}$$

Conservative divergence of normal vectors provides estimate of numerical curvature

$$\kappa = -\nabla \cdot \mathbf{n} \tag{13}$$

Due to smoothing momentum will not be fully conserved.

## Numerical curvature estimation : Youngs

Central, interfacial, cell and its eight neighbours used to determine normal vector.

Cell side volume fractions, $\alpha$, $\beta$, $\gamma$, $\delta$ are found from central and adjacent cells, based on three different types of PLIC interface configuration

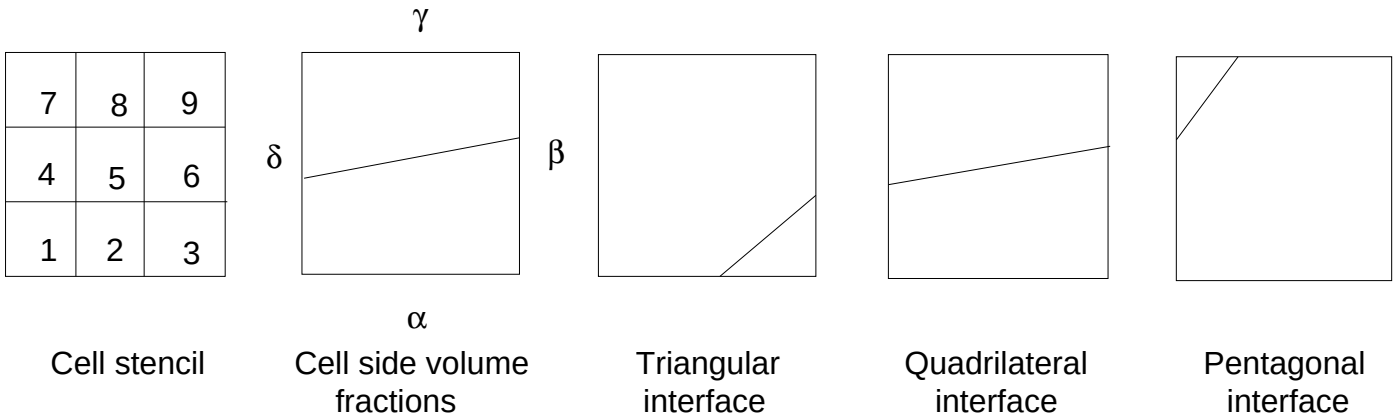

Corner values, $\{3, 5, 7, 9\}$ are used to detect cases where procedure fails

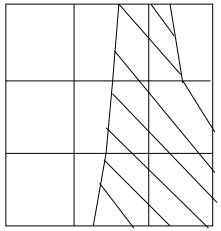

Simple differencing is used to calculate normal vector to the interface.

Numerical curvature estimated using (13).

## Numerical curvature estimation :: HF

In interface cells curvature calculated as such:

1. Calculate simple estimate of normal vector: $\mathbf{n} = -\nabla \mathbf{f}$

2. Orient height function in direction of maximal normal

3. Sum volume fractions to locally evaluate height function

   - If $|\mathbf{n_y}| > |\mathbf{n_x}|$ in cell (j,k) calculate $Y_{j-1,k}$, $Y_{j,k}$, $Y_{j+1,k}$

$$Y_{j,k} = \sum_{k-3}^{k+3} f_{j,k} \left( y_k - y_{k-1} \right) \tag{14}$$

4. Curvature follows from

$$\kappa = \frac{\mathbf{n_y}}{|\mathbf{n_y}|} \frac{Y_{xx}}{\left(1 + Y_x^2\right)^{3/2}} \tag{15}$$

5. $Y_x$, $Y_{xx}$ estimated using central differences

## Numerical curvature estimation : accuracy

A circle of radius $R = 2.0$ is centered at (1/2,1/2) in a unit square domain.

Exact curvature is $\kappa_{exact} = 1/R$.

Accuracy of methods determined via consideration of the following norm

$$L_\infty(|\kappa - \kappa_{\mathbf{exact}}|) = max(|\kappa - \kappa_{\mathbf{exact}}|) \tag{16}$$

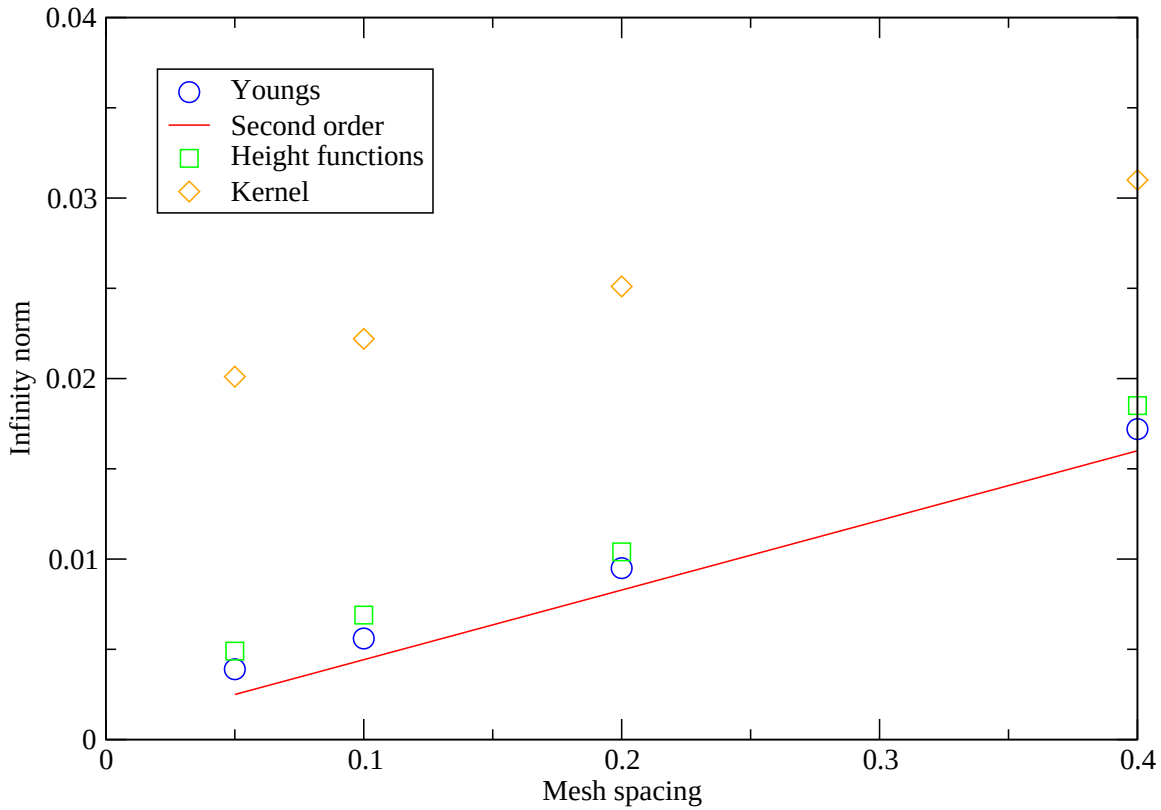


Method of Youngs implemented.

## Applications of the method: Static cylindrical drop

$\rho_{drop} = 1000$, $\rho_{back} = 1$, $\sigma = 73$

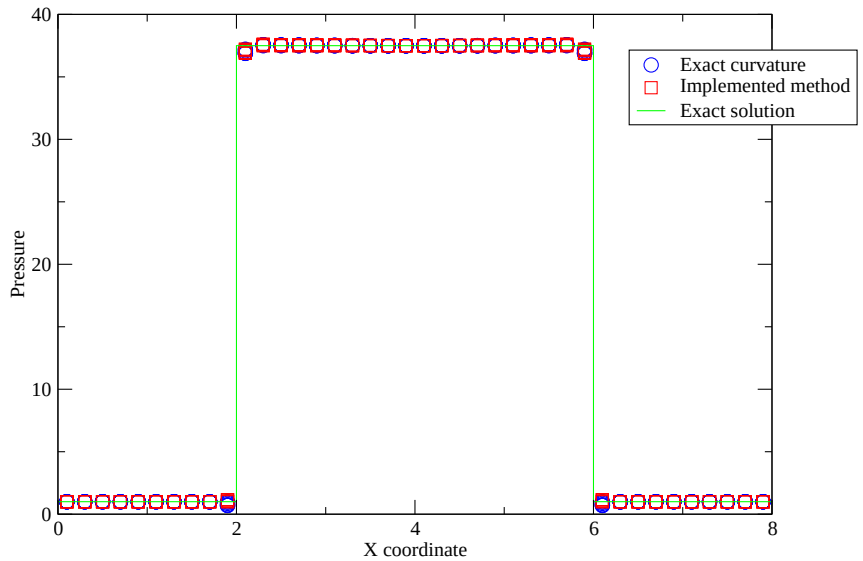


Computed pressure through the center of the static drop.

## Applications of the method: 2D Viscous droplet

An ellipsoidal drop $x^2/9 + y^2/4 = 1$ is placed in a 20 x 20 domain.

Fluid properties are $\rho_1 = 1$, $\rho_2 = 0.001$, $\mu_1 = 0.01$, $\mu_2 = 5\text{x}10^{-5}$, and $\sigma = 1$.

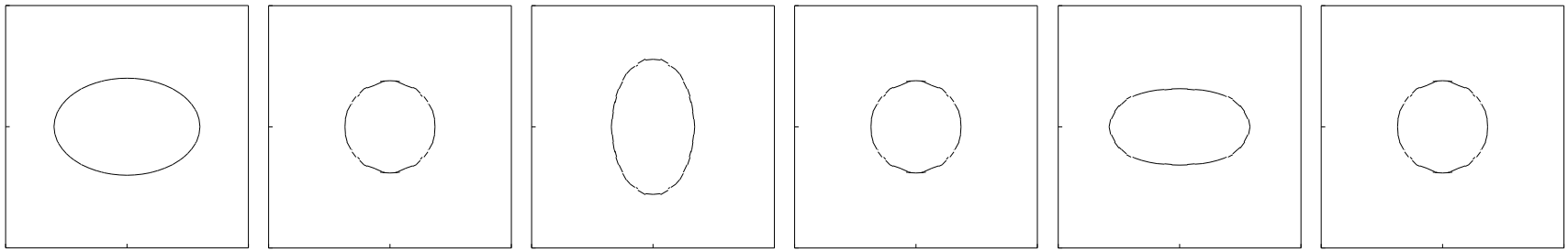

Evolution profile of 2D viscous droplet

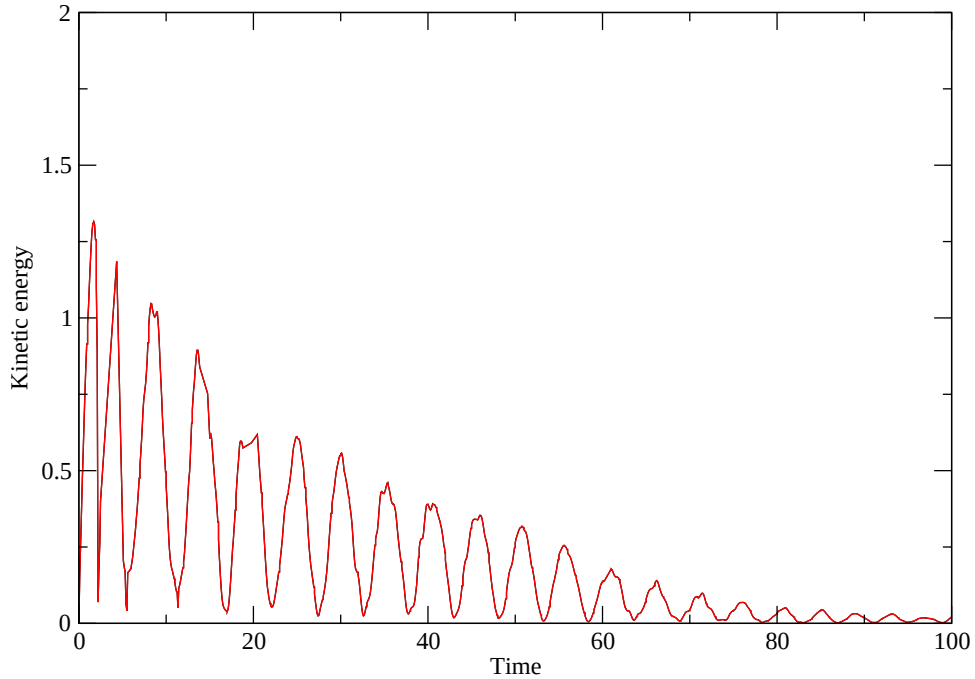


Kinetic energy V time profile for a 2D viscous droplet

$$\frac{|T_{theory} - T_{numerical}|}{T_{theory}} \times 100 < 2\%$$

## Applications of the method: Relaxation of a water filament

An axisymmetric domain of dimensions 7.0 mm x 1.0 mm contains a column of water with a bulbous elliptical end, sitting in a background of air.

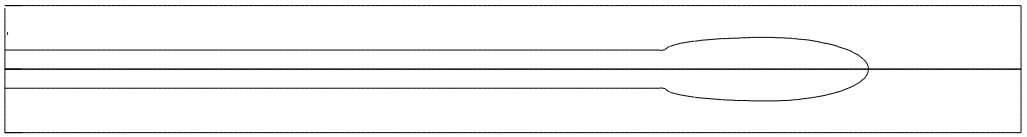

High curvature at rounded edges generates pressure gradients, which push fluid from the end towards the central stem of fluid, causing the bulbous end to swell.

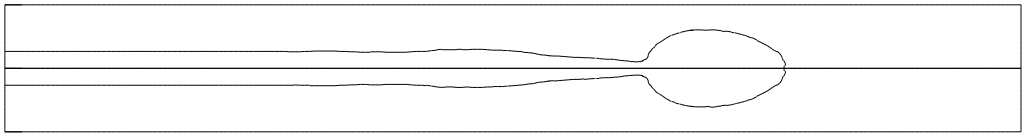

The bulbous end leads to a region of negative curvature and a minimum pressure, creating a necking region.

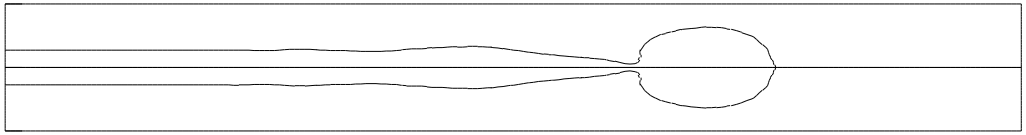

The necking region creates a region of high pressure gradients, which pushes fluid away from the neck in both directions, causing the reduction in radius of the neck, and eventual break off of the bulbous region.

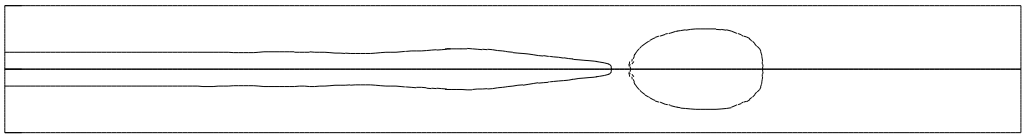

**Applications of the method: Rayleigh Taylor instability**

A heavy fluid, $\rho_1 = 3.0$, rests on top of a light fluid, $\rho_2 = 1.0$, in a gravitational field, $\mathrm{g} = 0.35$, supported by a counterbalancing pressure gradient.

A sinusoidal perturbation, wavelength 125 cm and amplitude 6.25 cm, is applied at the interface between the two fluids.

Linear mode analysis predicts an interfacial growth rate, $n$, given by

$$n^2 = \frac{2\pi}{\lambda(\rho_1 + \rho_2)} \left( \mathrm{g}(\rho_1 + \rho_2) - \sigma \left( \frac{2\pi}{\lambda} \right)^2 \right). \tag{17}$$

For a fixed wave-number a critical surface tension, $\sigma_c$, exists such that $n = 0$. A surface tension stability parameter is defined

$$\Phi(n) = \frac{\sigma}{\sigma_c} \tag{18}$$

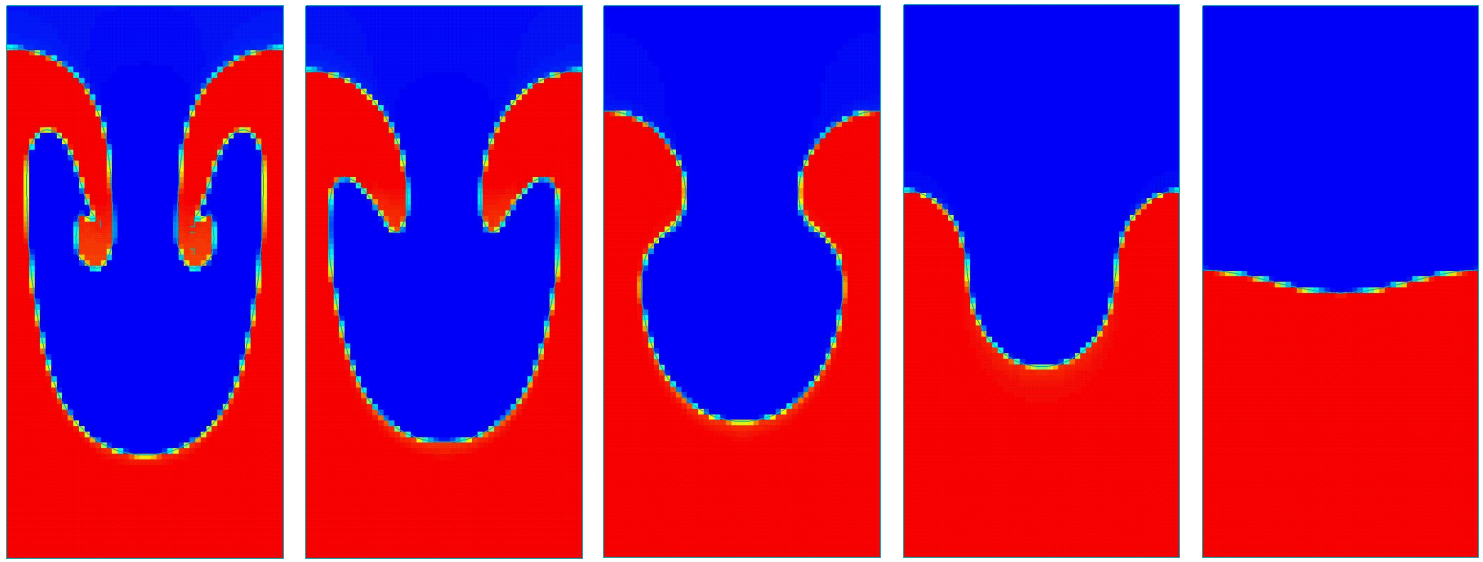

Interface plots at $t = 60$ for $\Phi = 0, 0.25, 0.5, 0.75, 0.75$ respectively.

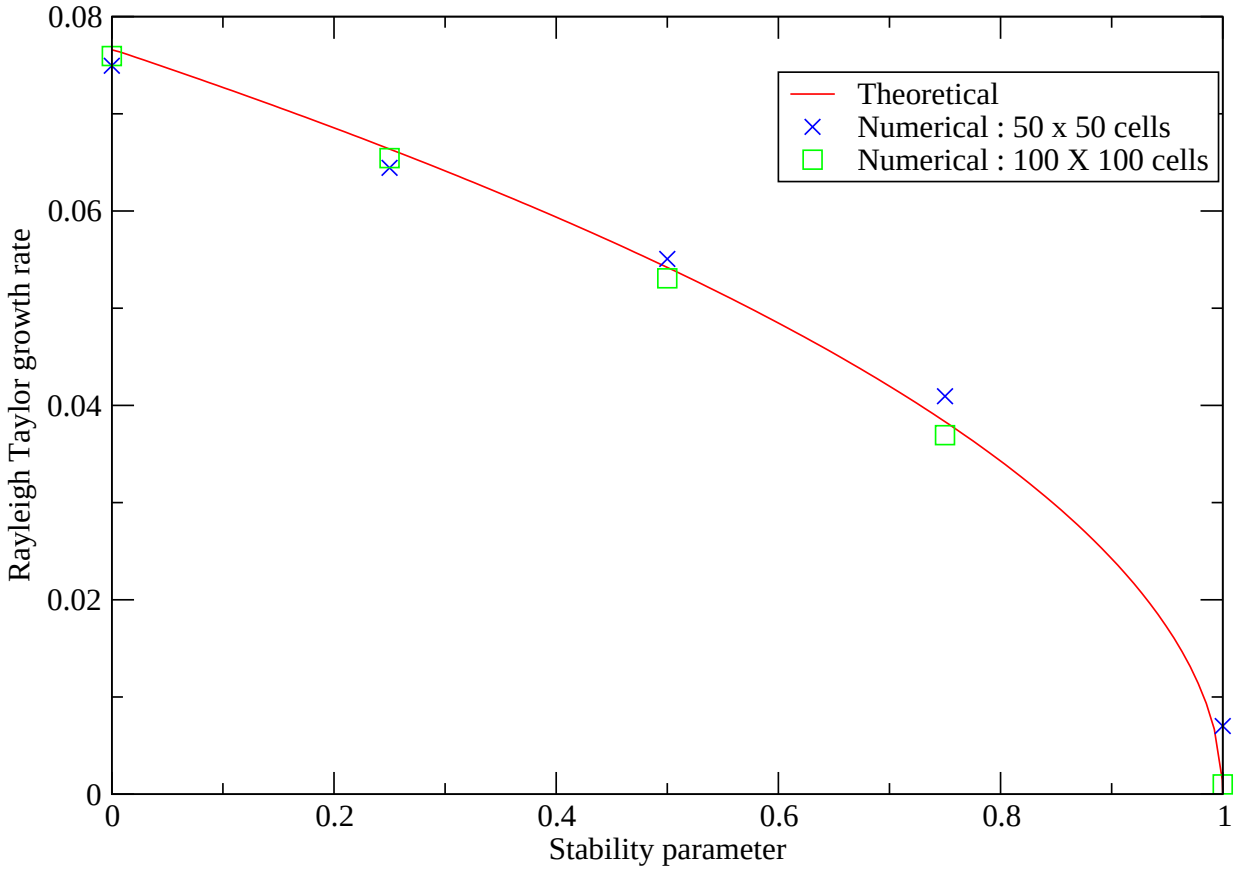


Growth rate : Numerical Vs Theoretical for RT instability.

## Conclusions

- A new discretization of the CSF model has been presented
- Only potential source of unphysical spurious currents lies within curvature estimation.
- The method is validated against the standard static drop test, viscous oscillating droplets, capillarity driven and fluid instability problems.
- The method copes well with a range of flows, of varying complexity.

# Bibliography

[1] J.U.Brackbill, D.B.Kothe, E.G.Puckett. A continuum method for modelling surface tension. *Journal of Computational Physics* 1992; **100**:335-354

[2] M.Francois, S.Cummins, E.Dendy, D.Kothe, J.Sicilian, M.Williams. A balanced-force algorithm for continuous and sharp interfacial surface tension models within a volume tracking algorithm. *Journal of Computational Physics* 2006; **213**:141-173

[3] D.B.Kothe, W.J.Rider, S.J.Mosso, J.S.Brock, J.I.Hochstein. Volume tracking of interfaces of interfaces having surface tension in two and three dimensions. In *Proceedings of the 34th Aerospace Sciences Meeting and Exhibit* 1996;

[5] D.L.Youngs. Time-dependent multi-material flow with large fluid distortion. In *Numerical Methods for Fluid Dynamics* K.W.Morton, M.J. Baines (eds) Academic press, 1982; 272–285.